# Thermoelectric performance of polyparaphenylene/$Li_{0.5}Ni_{0.5}Fe_2O_4$ nanocomposites prepared by mechanical ball mixing

WU ZIHUA, XIE HUAQING*, ZENG QINGFENG, YIN MING
*School of Urban Development and Environmental Engineering, Shanghai Second Polytechnic University, Shanghai 201209, P. R. China*

Polyparaphenylene/$Li_{0.5}Ni_{0.5}Fe_2O_4$ (PPP/LiNi-ferrite) nanocomposites were synthesized by mechanical ball mixing method and their thermoelectric properties were measured. With the increase of the PPP content, the electrical conductivity increase significantly. The thermal conductivity and lattice thermal conductivity of nanocomposite samples are smaller than those of pure LiNi-ferrite. Low thermal conductivity of the added PPP and the very large boundary between the conductive polymer and the oxide nanoparticles play dominant role on the thermal conductivity reduction. The figure of merit (*ZT*) of the PPP/LiNi-ferrite nanocomposite has been improved several orders in a wide temperature range from 300K to 800K. Fabrication of nanocomposites consisting of electrically conductive polymer and oxide nanoparticles may provide a promising way for realizing high-ZT thermoelectric performance.

(Received January 11, 2012; accepted April 11, 2012)

*Keywords:* Organic-inorganic nanocomposite, Thermoelectric property polyparaphenylene, $Li_{0.5}Ni_{0.5}Fe_2O_4$

## 1. Introduction

Thermoelectric (TE) materials provide unique capability to directly convert heat to electricity and provide spot cooling or heating [1]. Performance of these materials depends on a combination of Seebeck coefficient S, electrical conductivity $\sigma$, and thermal conductivity $\kappa$, consolidated into the thermoelectric figure of merit, $ZT = S^2\sigma T/\kappa$ [2,3]. Recent researches have made significant progress in the development of high-performance thermoelectric materials, but most are metallic or semi-metallic compounds like $BiTe_3$, PbTe and SiGe [4]. Certainly, the research mainstream is exploring thermoelectric materials with enhanced ZT values. However, some efforts have been also devoted to a search for the thermoelectric oxides, which have more advantages for the energy recovery applications, especially at elevated temperatures [5-7]. Although many metal oxides had been screened for high power factor, the *ZT* results were discouraging for the high thermal conductivity. In general, most oxides are known to be poor electrical conductors with low charge-carrier mobility and high thermal conductivity. These undesirable properties arise from the low mass of constituent atoms and the high vibration frequency of chemical bonds associated with $O^{2-}$ ions. Therefore, it is an important task to suppress this high $k$ without sacrificing the electrical properties [8-10]. Studies have shown that reduced thermal conductivity can be obtained in materials with high density of interfaces, which can be present in any geometry. Hence, a more promising approach is to fabricate nanocomposites which retain the high density of interfaces and can be produced using scalable and inexpensive processes. In this study, Polyparaphenylene/$Li_{0.5}Ni_{0.5}Fe_2O_4$ (PPP/ LiNi-ferrite) nanopowders were fabricated by mechanical ball milling method, and their thermoelectric properties were measured. The Seebeck coefficient is greatly improved while the electronic thermal conductivity is reduced resulting in an enhancement for the *ZT* values for the temperature range 300–800K. The conducting polymer PPP and LiNi-ferrite are chosen for the original materials. The LiNi-ferrite was selected as TE matrix because of the high Seebeck coefficient. Polyparaphenylene has high electrical conductivity and low thermal conductivity. Nanocomposite materials consisting of LiNi-ferrite and PPP may have much better TE properties than pure LiNi-ferrite. The electronic transport properties of the nanocomposite would be better than those of oxides, and the thermal conductivity would be lower because of the very low thermal conductivity of conducting polymers and the boundary between conducting polymers and the oxides particles. In addition, the chemical stability of polyparaphenylene in air at high temperature is in favor of the oxides for high-temperature thermoelectric power generation.

## 2. Experimental

LiNi-ferrite $Li_{0.5}Ni_{0.5}Fe_2O_4$ was prepared by a novel rheological phase reaction method [11]. In a typical procedure, stoichimetric amounts of $Li_2CO_3$ (0.01mol), $NiSO_4{\cdot}6H_2O$ (0.01mol), $Fe_2O_3$ (0.02mol) and $H_2C_2O_4{\cdot}2H_2O$ (0.084mol) were roughly mixed by grinding in an agate mortar for more than 30 min, about 15ml

anhydrous ethanol was then added to form the mixture in rheological state. The mixture was sealed in a teflonlined stainless-steel autoclave and maintained at 150℃ for 48 h in an oven. The obtained precursor was washed several times with deionized water and ethanol, dried at 60℃ for 10 h, and sintered at 1000℃ for 4 h in argon, followed by cooling in a furnace to room temperature with 5/min cooling rate. The most employed PPP synthesis method is developed by Kovacic which consists of polymerization of benzene in the presence of a catalyst, aluminum chloride ($AlCl_3$), and an oxidant, cupric chloride ($CuCl_2$) [12, 13]. The obtained powder exhibits a brown color. The obtained LiNi-ferrite and PPP powders were mixed with mechanical ball mixing and then consolidated by spark plasma sintering (SPS) at 735℃ for 10min under a pressure of 50MPa. The phase and composition of the products were characterized by X-ray diffraction (XRD) using a Rigaku D/max 2500 diffractometer at a voltage of 40 kV and a current of 200 mA with Cu-Kα radiation (λ=1.5406Å), employing a scanning rate 0.02 °/s in the 2θ ranging from 10 to 80°. The microstructure was examined by using a scanning electron microscope (SEM, Thermo Electron Corporation, A-6300). The thermal diffusivity ($\lambda$) was obtained by laser flash method (Anter, FL5000), and converted into thermal conductivity using $\kappa = \mathrm{d}\lambda C_p$, where d is the density of the sintered sample, and $C_p$ is the heat capacity. The lattice thermal conductivity $\mathrm{k}_\mathrm{L}$ was calculated from the Wiedemann-Franz relation, $\mathrm{k}_L = k - k_E$, where $k_E = L\sigma T$ is the electronic thermal conductivity, $L = 2.0\times10^{-8}V^2/K^2$ is the Lorentz number for a degenerate semiconductor, $\sigma$ is the electrical conductivity, $T$ is the temperature in Kelvin, and $k_L$ is the lattice thermal conductivity. The electrical conductivity ($\sigma$) and Seebeck coefficient (S) were measured using commercial equipment (ZEM-3, ULVAC-RIKO) on the bar-type sample with a dimension of 2mm×2mm in cross-section and 10mm in length.

## 3. Results and discussion

The X-ray diffraction patterns for PPP/LiNi-ferrite nanocomposite recorded at room temperature are shown in Fig. 1. The diffraction peaks and relative intensities of all patterns match well with a cubic spinel structure. The PPP is an amorphous nature showing no obvious diffraction peaks. No extra peaks of impurity phase were observed in the patterns which indicate that the powders obtained in the present work are single-phase nanoparticles.

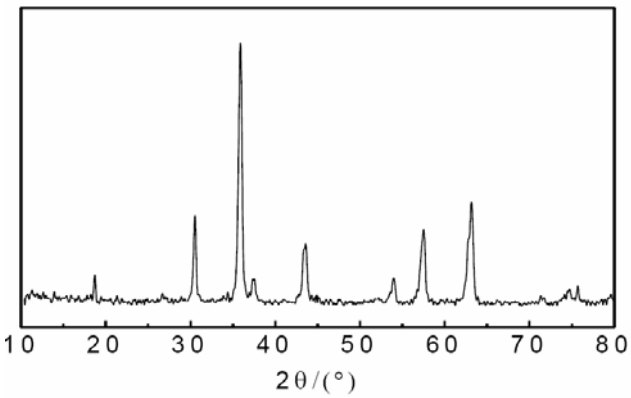


*Fig. 1 XRD patterns of PPP/LiNi-ferrite nanocomposite.*

The scanning electron microscopy (SEM) images in Fig. 2 represent the typical microstructures observed in the nanocomposite samples. It can be seen from Fig. 2 that there is irregular carpolite inside with dark contrast and outer with lighter contrast. The lighter-contrast area is PPP and the dark-contrast area is the polycrystalline of LiNi-ferrite. The image shows the LiNi-ferrite embedded in PPP with diffused boundaries. The nanosized grains of LiNi-ferrite are less than 250nm. LiNi-ferrite is an n-type semiconductor while the guest phase PPP is a p-type semiconductor. The electronic structures of the two phases are different from each other, which will create a potential at the phase interface. Electrons, which are the dominant carriers in the nanocomposite, have to overcome a potential at the interface. The electron of low energy (with small relaxation time) is filtered by such extra potential, leading to a local increase in electron number at the Fermi level [14,15]. Both energy-barrier scattering and a distortion of the electronic density of states are useful for reducing thermal conductivity.

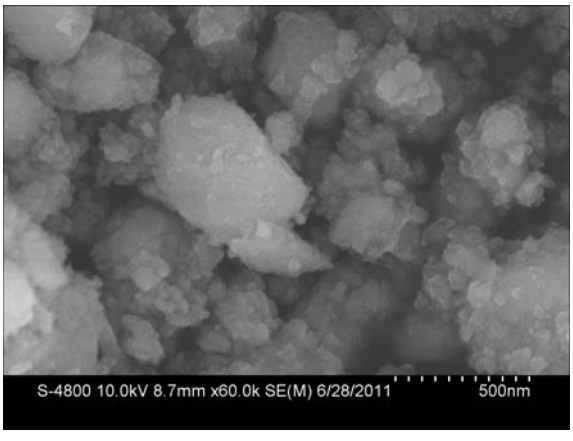


*Fig. 2 SEM micrographs of PPP/LiNi-ferrite nanocomposites.*

The variations of electrical conductivity of the PPP/LiNi-ferrite nanocomposite samples with temperature are shown in Fig. 3. The pure LiNi-ferrite sample that was sintered under the same condition with PPP/LiNi-ferrite nanocomposite exhibits low electrical conductivity as a few mS/m. The electrical conductivity of the pure LiNi-ferrite is almost constant in the temperature range. Compared with the pure LiNi-ferrite, the electrical conductivities of the PPP/LiNi-ferrite nanocomposite increased substantially and show a significant increase with measuring temperature. With the addition of 0.8wt% PPP, the electrical conductivity at 750K became higher by > 5 orders of magnitude than that of pure LiNi-ferrite. The electrical conductivity of PPP/LiNi-ferrite nanocomposite shows a monotonic increase with increase in PPP content. We have not got the intrinsic electronic transport properties of PPP, because the PPP is hard to make into flake. Ueno et al studied the electrical conductivity of PPP film and found the electrical conductivity may reach 400~500 S/cm [16]. The density of the samples may affect the measured electrical conductivity. Porosity correction to 100% theoretical density is performed by using the following Maxwell-Eucken equation [17]:

$$\sigma = \sigma_{\mathrm{m}}(1+2\phi_{\mathrm{p}}\mathrm{A})/(1-\phi_{\mathrm{p}}\mathrm{A}) = [3/(1-\phi_{\mathrm{p}}\mathrm{A})-2]\sigma_{\mathrm{m}} \quad (1)$$

$$\mathrm{A} = (1-\sigma_{\mathrm{m}}/\sigma_{\mathrm{p}})(2\sigma_{\mathrm{m}}/\sigma_{\mathrm{p}}+1) \quad (2)$$

where $\sigma$ is the electrical conductivity of the dense material, and $\phi$ is the fraction (subscript m indicates matrix, and p indicates particle). Because the electrical conductivity of PPP is larger than that of LiNi-ferrite, there is $\sigma_{\mathrm{m}}/\sigma_{\mathrm{p}}<1$ and then A>0. It can be seen from Eq. (1) that the electrical conductivity of nanocomposite increases with increasing PPP content. These results are consistent with the experiment results shown in Fig. 3. With the increase of the PPP content, the electrical conductivity increase more significantly.

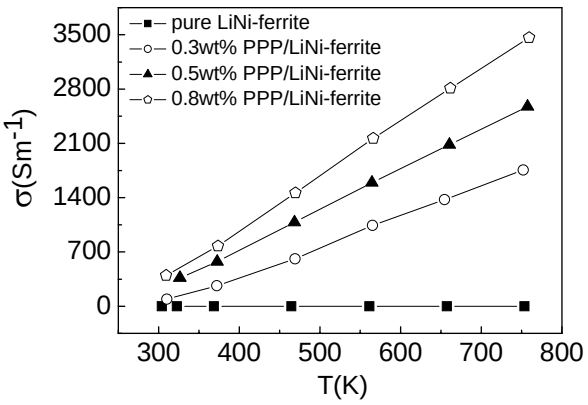


*Fig. 3 Temperature dependences of electrical conductivity for the PPP/LiNi-ferrite nanocomposite with changing of PPP content.*

Fig. 4 shows the Seebeck coefficient as a function of temperature for pure LiNi-ferrite and PPP/LiNi-ferrite nanocomposite. The negative values of Seebeck coefficient indicate that all the samples are n-type semiconductor and the major carrier is electron. The pure LiNi-ferrite sample presented a high Seebeck coefficient of about -315μV/K. The Seebeck coefficient of pure LiNi-ferrite sample is almost constant in the temperature range. The Seebeck coefficient of PPP/LiNi-ferrite nanocomposite decreases with decreasing temperature below 400K and then decreases with increasing temperature above 400K. The absolute values of Seebeck coefficient for PPP/LiNi-ferrite nanocomposite decrease with increase in the mixing content of PPP. According to the Ioffe theory, the Seebeck coefficient is inversely proportional to the carrier concentration. As discussed above, the carrier concentration increases due to the mixing of PPP [18].

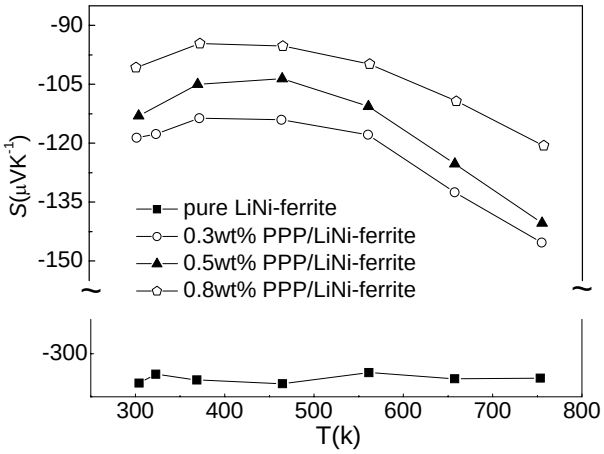


*Fig. 4 Temperature dependences of Seebeck coefficient for the PPP/LiNi-ferrite nanocomposite with changing of PPP content*

Fig. 5 shows the thermal conductivity and lattice thermal conductivity of PPP/LiNi-ferrite nanocomposite. It is clear that the thermal conductivity of PPP/LiNi-ferrite nanocomposite is much lower than that of the pure LiNi-ferrite. It is well known that the thermal conductivity can be varied greatly by extrinsic factor such as microstructure and impurities. The overall $\kappa$ value of a solid is given as $\kappa = \kappa_{\mathrm{L}} + \kappa_{\mathrm{E}}$. As shown in Fig. 5, it is confirmed that the lattice thermal conductivity $\kappa_{\mathrm{L}}$ has a dominate proportion relative to the electron thermal conductivity, which is estimated by the Wiedeman- Franz relation. The thermal conductivity value of pure LiNi-ferrite is about 7 $\mathrm{Wm^{-1}K^{-1}}$ at room temperature and decreased to about 2.5 $\mathrm{Wm^{-1}K^{-1}}$ at 1000 K. The thermal conductivity also decreased with increase in amount of PPP. The thermal conductivity of PPP/LiNi-ferrite nanocomposite decreases as the temperature increases. Marked reduction in the lattice thermal conductivity was observed in the nanocomposite, and lattice thermal

conductivity decreases with increasing PPP content for samples. Nanostructuring of bulk materials has led to significant improvements in ZT as engineering nanoscale interfaces introduce possibilities for both phonon scattering and the energy-dependent scattering of electrical carries [19-22]. Due to the high density of interfaces and grain boundaries present in the nanocomposites, the scattering of phonons across a broad wavelength spectrum was enhanced. This suppressed the lattice thermal conductivity of the nanocomposites significantly. In addition, the drastic difference of vibrational states in the two components would reduce the thermal transition. Consequently, the nanocomposites exhibited an average low $\kappa_L$.

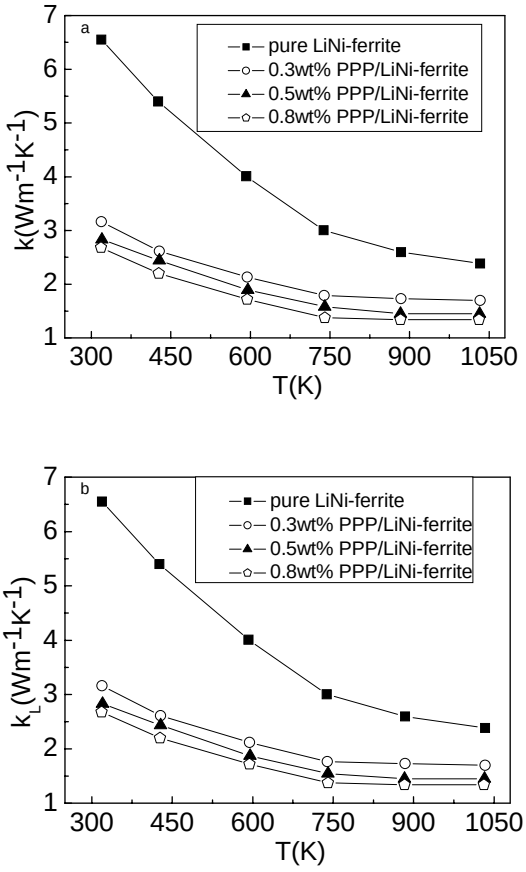


*Fig. 5 Temperature dependences of thermal conductivity (a) and lattice thermal conductivity (b) for the PPP/LiNi-ferrite nanocomposite with changing of PPP content*

The temperature dependence of the dimensionless figure of merit, ZT, is shown in Fig. 6. Because of the combined effects of increased electrical conductivity and reduced thermal conductivity, the PPP/LiNi-ferrite nanocomposite show considerably larger values than pure LiNi-ferrite. In the present temperature range investigated, the ZT value reached 0.028 at 800K in the 0.8wt% PPP/LiNi-ferrite nanocomposite, which show a trend to further increase at higher temperatures. This result indicates a possibility to further improve the thermoelectric performance of PPP/LiNi-ferrite nanocomposite through processing modification.

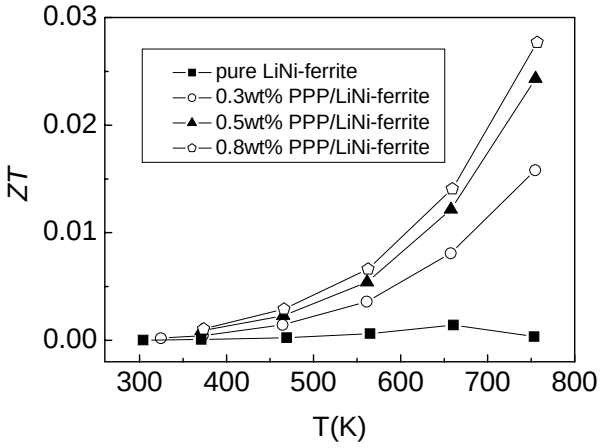


*Fig. 6 Temperature dependences of the figure of merit for the PPP/LiNi-ferrite nanocomposite with changing of PPP content*

## 4. Conclusions

PPP/LiNi-ferrite nanocomposites were synthesized by mechanical ball mixing method and their thermoelectric properties were measured. The XRD pattern of LiNi-ferrite shows the single phase spinel structure with the characteristic reflections of the Fd3m cubic spinel group. With the increase of the PPP content, the electrical conductivity increase significantly. Absolute values of Seebeck coefficient for nanocomposites decrease with increase of content of PPP. The decrease of the Seebeck coefficient is mainly caused by the low Seebeck coefficient of PPP. The thermal conductivity and lattice thermal conductivity of nanocomposite samples are smaller than those of pure LiNi-ferrite. Due to the high density of interfaces and grain boundaries present in the nanocomposites, the scattering of phonon across a broad wavelength spectrum was enhanced. This suppressed the lattice thermal conductivity of the nanocomposites significantly. The analysis of both the electrical and thermal transport properties shows that the increased electrical conductivity and reduced lattice thermal conductivity lead to a notable enhancement of ZT value for the whole temperature range. It is expected that much higher ZT values would be obtained if the temperature is further increased.

**Acknowledgments**

This work was supported by the Program for New Century Excellent Talents in University (NCET-10-883) and Program for Professor of Special Appointment (Eastern Scholar) at Shanghai Institutions of Higher Learning.

## References

[1] L.E. Bell, Science, **21,** 1457, (2008).
[2] G. J.Snyder, E. S. Toberer, Nat. Mater. **7**, 105 (2008).
[3] G. Q. Zhang, Q. X. Yu, W. Wang, X. G. Li, Adv. Mater. **22**, 1959 (2010).
[4] G. Chen, M.S. Dresselhaus, G. Dresselhaus, J. P. Fleurial, T. Caillat, Int. Mater. Rev. **48**, 45 (2003).
[5] H. Ohta, S. Kim, Y. Mune, T. Mizoguchi, K. Nomura, S. Ohta, T. Nomura, Y. Nakanishi, Y. Ikuhara, M. Hirano, H. Hosono, K. Koumoto, Nat. Mater. **6**, 129 (2007).
[6] I. Terasaki,Y. Sasago, K. Uchinokura, Phys. Rev. B **56**, R12685 (1997).
[7] H. Q. Liu, Y. Song, S. N. Zhang, X. B. Zhao, F. P. Wang, J. Phys. Chem. Solids **70** 600 (2009).
[8] T. Tsubota, M. Ohtaki, K. Eguchi, H. Arai, J. Mater. Chem. **7**, 85 (1997).
[9] G. A. Slack, Phys. Rev. B **6**, 3791 (1972).
[10] T. Tsubota, M. Ohtaki, K. Eguchi, H. Arai, J. Mater. Chem. **8**, 409 (1998).
[11] L. C. Li, J. Jiang, F. Xu, J. Mater. Lett. **61**, 1091 (2007).
[12] P. Kovacic, A. Kyriakis, J. Am. Chem. Soc. **85,** 454 (1963).
[13] P. Kovacic, F. W. Koch, J. Org. Chem. **28,** 1864 **(**1963**)**.
[14] Z. Xiong, X. H.Chen, X. Y.Huang, S. Q.Bai, L. D. Chen, Acta Mater. **58**, 3995 (2010).
[15] Y. Z. Pei, A. Andrew, G. J. Snyder, Adv. Energy Mater. **1**, 291 (2011).
[16] H. Ueno, K. Yoshino, Phys. Rev. B **34,** 7158 (1986).
[17] B. Zhang, J. Sun, H. E. Katz, F. Fang, R. L. Opila, ACS Appl. Mater. & inter. **2,** 3170 (2010).
[18] A.F. Ioffe, Semiconductor Thermoelements and Thermoelectric Cooling, Infosearch Ltd. Press, London (1957).
[19] W. Kim, J. Zide, A. Gossard, D. Klenov, S. Stemmer, Phys. Rev. Lett. **96,** 045901 (2006).
[20] E. T. Swartz, R. O. Pohl, Rev. Mod. Phys. **61**, 605 (1989).
[21] J. C. Grunlan, Y. S. Kim, S. Ziaee, X. Wei, B. A. Magid, K. Tao, Macromol. Mater. Eng. **291**, 1035 (2006).
[22] L. Liu, J. C. Grunlan, Adv. Funct. Mater. **17,** 2343 (2007).

*Corresponding author: hqxie@eed.sspu.cn